Journal of Materials Chemistry A

PAPER

Study on the cycling performance of $LiNi_{0.5}Mn_{1.5}O_4$ electrodes modified by reactive SiO_2 nanoparticles†

Cite this: J. Mater. Chem. A, 2014, 2, 6863

Won-Kyung Shin, Yoon-Sung Lee and Dong-Won Kim*

We demonstrate a facile approach to improve the cycling stability of spinel $LiNi_{0.5}Mn_{1.5}O_4$ materials by their surface modification. The cross-linked composite polymer electrolyte layer was formed on the surface of $LiNi_{0.5}Mn_{1.5}O_4$ by radical polymerization between diethylene glycol diacrylate and SiO_2 nanoparticles with reactive vinyl groups. The protective composite polymer layer formed on the $LiNi_{0.5}Mn_{1.5}O_4$ materials suppressed the irreversible decomposition of the electrolyte at high voltages and reduced the dissolution of transition metals from the charged $LiNi_{0.5}Mn_{1.5}O_4$ electrode into the electrolyte at elevated temperature, which resulted in more stable cycling characteristics than the pristine $LiNi_{0.5}Mn_{1.5}O_4$ electrode.

Received 7th November 2013
Accepted 21st February 2014

DOI: 10.1039/c3ta14558a

www.rsc.org/MaterialsA

Introduction

The rapidly expanding use of rechargeable lithium batteries in power sources for portable electronic devices, electric vehicles and energy storage systems has heightened the need for high energy density and enhanced safety of the batteries.[1–3] To achieve high energy density, many researchers have developed high voltage cathode materials with high reversible capacities.[4] In particular, a great deal of attention has focused on the spinel-structured $LiNi_{0.5}Mn_{1.5}O_4$ material because of its high theoretical capacity (~147 mA h g^{-1}), high operating voltage and good rate capability.[5–8] However, this material still has issues to be addressed. These issues include oxidative decomposition of the electrolyte at high voltages and dissolution of transition metals (Mn, Ni) into the electrolyte, particularly at elevated temperatures, which can lead to gradual deterioration of cell performance upon cycling. Numerous approaches to solve these problems have been proposed, such as new electrolyte systems that exhibit high anodic stability,[9,10] the addition of various additives to the electrolyte,[11] and surface coating with metal oxides[12–15] or polymers.[16,17] In particular, the surface modification of $LiNi_{0.5}Mn_{1.5}O_4$ has proven highly effective for mitigating interfacial side reactions between $LiNi_{0.5}Mn_{1.5}O_4$ and liquid electrolytes at high voltages, as well as for suppressing the dissolution of transition metal ions at elevated temperatures. In our previous studies, we synthesized silica nanoparticles with C=C double bonds, which permitted the surface reaction with vinyl monomers by radical polymerization.[18–20] Encouraged by previous studies, the surface modification of $LiNi_{0.5}Mn_{1.5}O_4$ with inorganic SiO_2 nanoparticles containing reactive groups is of great interest because the $LiNi_{0.5}Mn_{1.5}O_4$ particles can be entirely covered with a composite polymer synthesized by radical polymerization between SiO_2 particles and a vinyl monomer.

In the present study, the reactive SiO_2 nanoparticles were uniformly dispersed on the surface of $LiNi_{0.5}Mn_{1.5}O_4$ materials in order to induce the cross-linking reaction on their surface. The $LiNi_{0.5}Mn_{1.5}O_4$ active materials were then effectively wrapped by a chemical cross-linking reaction between reactive SiO_2 nanoparticles and diethylene glycol diacrylate (DEGDA). The effect of surface modification with reactive SiO_2 particles on the cycling performance of the $LiNi_{0.5}Mn_{1.5}O_4$ electrode is reported.

Experimental

Synthesis of reactive SiO_2 nanoparticles

SiO_2 nanoparticles with reactive vinyl groups were synthesized, as reported previously.[18–20] Briefly, 2 ml of vinyltrimethoxysilane (VTMS, Sigma-Aldrich) was added to 150 ml of double distilled water, which was then stirred until the VTMS droplets completely disappeared. Next, 10 ml of an NH_4OH solution (28 wt%) was added to the solution, and the reaction was maintained for 4 h at 70 °C. After completion of the reaction, the resulting precipitate was centrifuged and washed several times with ethanol. The resulting SiO_2 nanoparticles were dried under vacuum at 110 °C for 12 h.

Electrode preparation and cell assembly

The $LiNi_{0.5}Mn_{1.5}O_4$ active materials were kindly supplied by Samsung SDI. The reactive SiO_2 nanoparticles corresponding to

Department of Chemical Engineering, Hanyang University, Seungdong-Gu, Seoul 133-791, Republic of Korea. E-mail: dongwonkim@hanyang.ac.kr; Fax: +82 2 2220 4337; Tel: +82 2 2220 2337

† Electronic supplementary information (ESI) available. See DOI: 10.1039/c3ta14558a

1, 2, 3 and 4 wt% of $LiNi_{0.5}Mn_{1.5}O_4$ powders were dispersed in ethanol by sonication for 1 h. The $LiNi_{0.5}Mn_{1.5}O_4$ powders were then added to the above colloid solution; the resulting solution was stirred by a magnetic stirrer for 2 h and subsequently filtered. After filtering, the active materials were dried at 50 °C for 12 h and further dried under vacuum at 110 °C for 12 h, which resulted in homogeneous dispersion of reactive SiO_2 nanoparticles on the surface of the $LiNi_{0.5}Mn_{1.5}O_4$ active materials. The $LiNi_{0.5}Mn_{1.5}O_4$ electrode was prepared by coating an *N*-methyl pyrrolidone (NMP)-based slurry containing 85 wt% $LiNi_{0.5}Mn_{1.5}O_4$ active materials decorated with reactive SiO_2 nanoparticles, 7.5 wt% poly(vinylidene fluoride) (PVdF) and 7.5 wt% Super P carbon (MMM Co.) onto an Al foil. The electrode was dried under vacuum at 110 °C for 12 h. Its active mass loading corresponded to a capacity of approximately 1.0 mA h cm^{-2}. The lithium electrode consisted of a 100 μm-thick lithium foil (Honjo Metal Co., Ltd) that was pressed onto a copper current collector.

To prepare the gel electrolyte precursor, 4 wt% of DEGDA (Sigma-Aldrich) was dissolved in the liquid electrolyte with azobisisobutyronitrile (Sigma-Aldrich, 0.5 wt% of DEGDA) as a thermal radical initiator. The liquid electrolyte used was 1 M $LiPF_6$ in ethylene carbonate (EC)–diethyl carbonate (DEC)–ethyl methyl carbonate (EMC) (3 : 5 : 2 by volume, battery grade, Soulbrain Co., Ltd). The CR2032-type coin cell composed of the lithium electrode, microporous polyethylene separator (Asahi, ND 420) and $LiNi_{0.5}Mn_{1.5}O_4$ electrode was assembled with a gel electrolyte precursor. All cells were assembled in a dry box filled with argon gas. After the cell assembly, the cells were stored at 90 °C for 20 min to induce the *in situ* chemical cross-linking reaction between the gel electrolyte precursor and reactive SiO_2 nanoparticles on the surface of the $LiNi_{0.5}Mn_{1.5}O_4$ powder.

Measurements

The morphologies of the SiO_2 nanoparticles and $LiNi_{0.5}Mn_{1.5}O_4$ electrode were examined using a field emission scanning electron microscope (FE-SEM, JEOL JSM-6330F). Fourier transform infrared (FT-IR) spectra were recorded on a Magna IR 760 spectrometer in the range of 400–4000 cm^{-1} with KBr powder-pressed pellets. Powder X-ray diffraction (XRD) (Rigaku, Rint-2000) using Cu Kα radiation was used to identify the crystalline phase of the pristine and SiO_2-modified $LiMn_{1.5}Ni_{0.5}O_4$ powders. Charge and discharge cycling tests of the Li/$LiNi_{0.5}Mn_{1.5}O_4$ cells were conducted at a current density of 0.5 mA cm^{-2} (0.5 C rate) over a voltage range of 3.0–4.9 V using battery testing equipment (WBCS 3000, Wonatech). AC impedance measurements were performed using a Zahner Electrik IM6 impedance analyzer over the frequency range of 1 mHz to 100 kHz with an amplitude of 10 mV. For the quantitative measurement of transition metal ion dissolution, the fully charged cells were carefully disassembled to obtain the charged $LiNi_{0.5}Mn_{1.5}O_4$ electrodes. These electrodes were stored in the fresh liquid electrolyte at 55 °C. The dissolved transition metal content in the liquid electrolyte was then measured as a function of storage time using atomic absorption spectroscopy (AA, Vario 6, Analytik Jena).

Results and discussion

Fig. 1(a) presents the FE-SEM image of reactive SiO_2 particles. The silica particles have a uniform spherical shape with an average diameter of 230 nm. The chemical structure of the reactive SiO_2 particles was confirmed by the FT-IR spectrum, as presented in Fig. 1(b). From the FT-IR spectrum, peaks corresponding to the siloxane (Si–O–Si) group (766, 1000–1200 cm^{-1}) and C=C double bonds (1410, 1603 cm^{-1}) were observed. This result implies that the SiO_2 particles contain reactive vinyl groups, which permit further radical polymerization with DEGDA.

Fig. 2(a) shows a photograph of the cross-linked gel polymer electrolyte prepared with the gel electrolyte precursor containing DEGDA. The electrolyte solution became non-fluidic after thermal cross-linking because of the formation of three dimensional networks. The FT-IR spectra of the gel-electrolyte precursor and cross-linked gel polymer electrolyte shown in Fig. 2(b) reveal that the C=C double bond peaks observed at 1634 and 1616 cm^{-1} completely disappeared after chemical-cross-linking. This result confirms that DEGDA was polymerized to form the cross-linked polymer by radical polymerization.

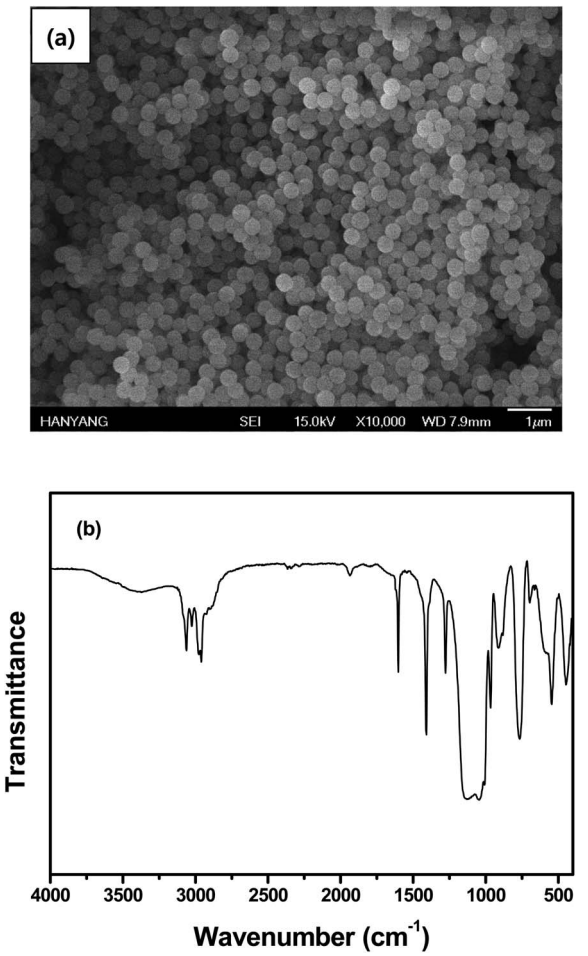

Fig. 1 (a) SEM image and (b) FT-IR spectrum of reactive SiO_2 nanoparticles.

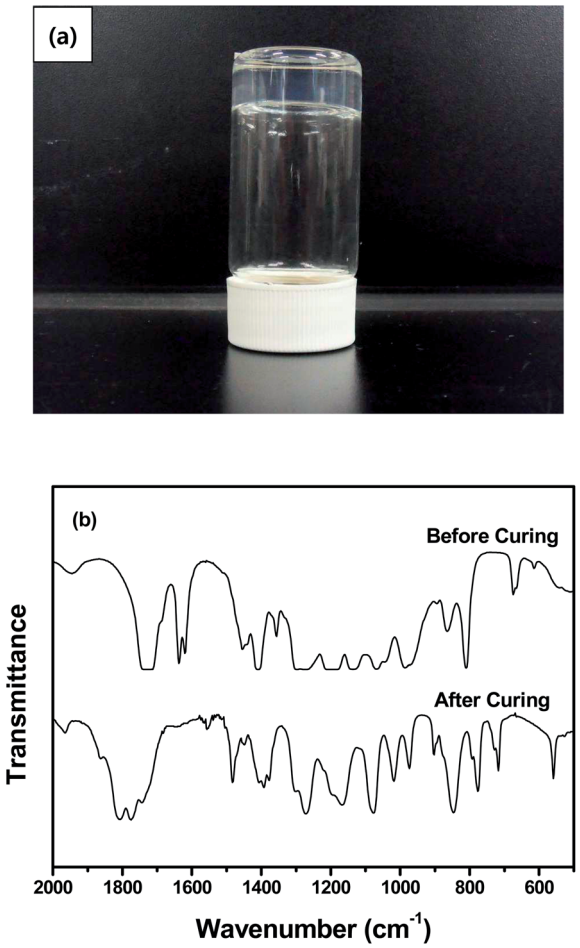

Fig. 2 (a) Photograph of the gel polymer electrolyte, and (b) FT-IR spectra of a gel electrolyte precursor (before curing) and gel polymer electrolyte (after curing).

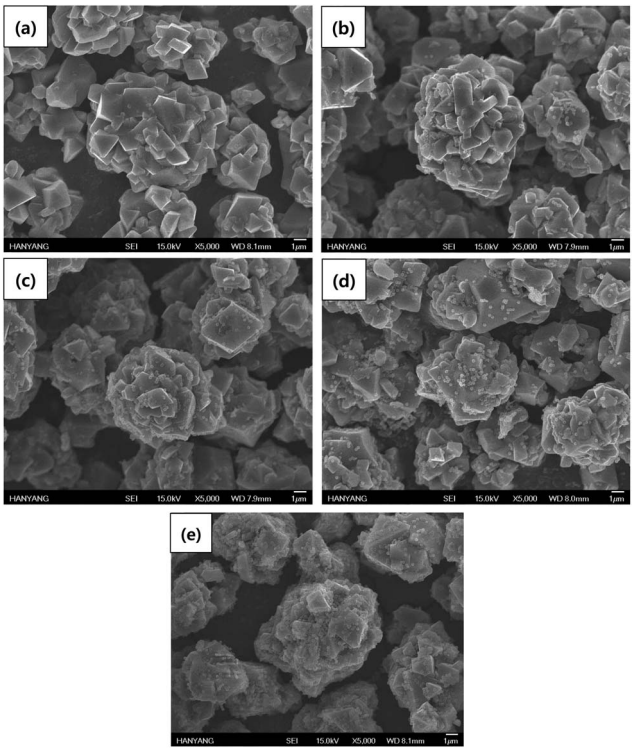

Fig. 3 SEM images of (a) pristine $LiNi_{0.5}Mn_{1.5}O_4$ materials, and SiO_2-decorated $LiNi_{0.5}Mn_{1.5}O_4$ materials with SiO_2 nanoparticles of (b) 1 wt%, (c) 2 wt%, (d) 3 wt% and (e) 4 wt%.

FE-SEM images of the $LiNi_{0.5}Mn_{1.5}O_4$ active materials with and without reactive SiO_2 nanoparticles are presented in Fig. 3. As shown in Fig. 3(b)–(e), the nano-sized SiO_2 particles were uniformly distributed on the surface of the $LiNi_{0.5}Mn_{1.5}O_4$ active material without agglomeration. As the content of reactive SiO_2 nanoparticles increased, a large number of nanoparticles were observed on the surface of the $LiNi_{0.5}Mn_{1.5}O_4$ powder. Because the SiO_2 nanoparticles contain a lot of reactive vinyl groups, they would participate in radical polymerization with DEGDA on the surface of the active $LiNi_{0.5}Mn_{1.5}O_4$ material. Accordingly, the active $LiNi_{0.5}Mn_{1.5}O_4$ materials are expected to be effectively wrapped by the composite polymer layer formed with DEGDA and reactive SiO_2 particles, as schematically demonstrated in Fig. 4. XRD patterns for the pristine and SiO_2-modified $LiNi_{0.5}Mn_{1.5}O_4$ powders are compared in Fig. S1.† All of the diffraction patterns can be assigned to a spinel structure indexed by cubic *Fd*3*m* in which lithium ions occupy the tetragonal (8a) sites, transition metals (Mn and Ni) are located at the octahedral (16d) sites, and oxygen atoms reside in 32e sites.[21] No significant differences in the XRD patterns between the pristine and SiO_2-modified $LiNi_{0.5}Mn_{1.5}O_4$ powders were observed. This result demonstrates that the surface modification of the $LiNi_{0.5}Mn_{1.5}O_4$ powders using the reactive SiO_2 particles has no influence on the crystal structure of the host materials.

Fig. 5 presents cross-sectional FE-SEM images of $LiNi_{0.5}Mn_{1.5}O_4$ electrodes with and without reactive SiO_2 nanoparticles (3 wt%), which were obtained after cross-linking with the gel electrolyte precursor containing DEGDA. The pristine $LiNi_{0.5}Mn_{1.5}O_4$ active materials exhibited well-defined edges, as shown in Fig. 5(a). In contrast, the $LiNi_{0.5}Mn_{1.5}O_4$ active materials with reactive SiO_2 nanoparticles were more effectively enwrapped with a cross-linked composite polymer layer containing SiO_2 nanoparticles, which were formed by a cross-linking reaction between reactive SiO_2 particles and DEGDA. This result suggests that SiO_2 particles with vinyl groups play a role as effective cross-linking sites on the surface of $LiNi_{0.5}Mn_{1.5}O_4$ active materials in the positive electrode during thermal cross-linking, as schematically illustrated in Fig. 4. Compared to conventional metal oxide-based coatings yielding discontinuous deposition of an electrically inert layer, the composite polymer layer has the distinctive features of completely covering the $LiNi_{0.5}Mn_{1.5}O_4$ active materials and possessing ionic conductivity for transport of Li^+ ions. As shown in Fig. S2,† the ionic conductivities of the composite polymer layer ranged from 6.8 to 7.9 mS cm^{-1}, and decreased with the SiO_2 content due to the increase of cross-linking density. The enhanced interfacial adhesion between $LiNi_{0.5}Mn_{1.5}O_4$ active materials and the gel polymer electrolyte in the positive electrode was also expected during *in situ* chemical cross-linking in the cell.

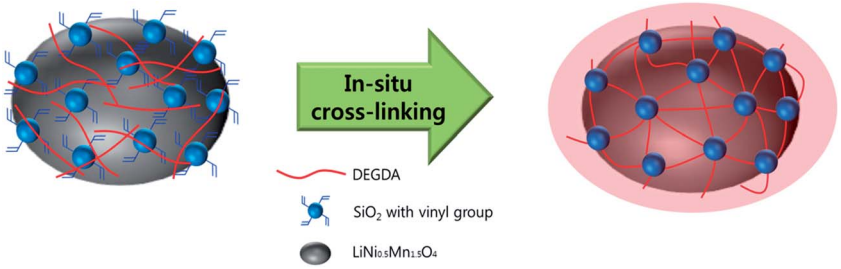

Fig. 4 Schematic illustration for synthesis of a composite polymer layer on the surface of $LiNi_{0.5}Mn_{1.5}O_4$ powder using reactive SiO_2 nanoparticles and DEGDA.

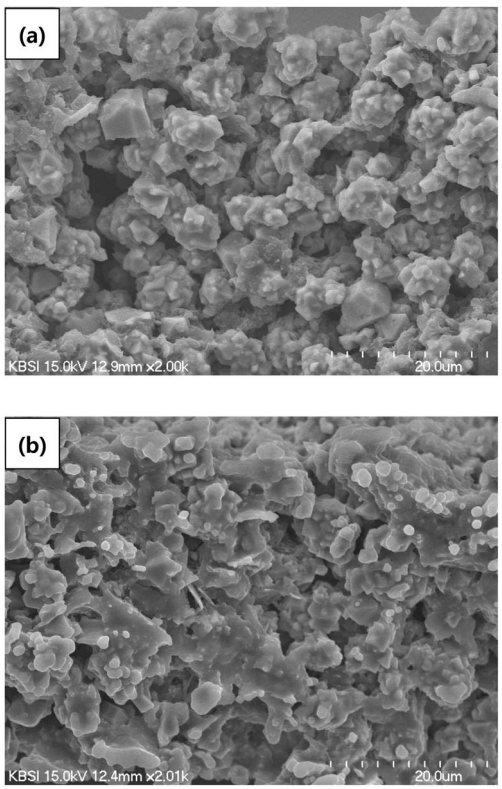

Fig. 5 Cross-sectional SEM images of the (a) pristine $LiNi_{0.5}Mn_{1.5}O_4$ electrode and (b) SiO_2-decorated $LiNi_{0.5}Mn_{1.5}O_4$ electrode (3 wt% SiO_2) after cross-linking with the gel electrolyte precursor at 90 °C for 20 min.

The cycling performance of $Li/LiNi_{0.5}Mn_{1.5}O_4$ cells assembled with the pristine $LiNi_{0.5}Mn_{1.5}O_4$ electrode and SiO_2-modified $LiNi_{0.5}Mn_{1.5}O_4$ electrode was evaluated. The cells were charged at a current density of 0.1 mA h cm^{-1} (0.1 C rate) up to a target voltage of 4.9 V. The cells were then discharged to a cut-off voltage of 3.0 V at the same current density. Fig. 6 shows the charge/discharge curves of the $Li/LiNi_{0.5}Mn_{1.5}O_4$ cells with and without reactive SiO_2 nanoparticles (3 wt%). The cell with pristine $LiNi_{0.5}Mn_{1.5}O_4$ electrodes delivered an initial discharge capacity of 131.8 mA h g^{-1}, based on the active $LiNi_{0.5}Mn_{1.5}O_4$ material in the positive electrode, and a coulombic efficiency of 85.2%. In contrast, the cell assembled with 3 wt% reactive SiO_2 particles showed a similar initial discharge capacity (130.7 mA h g^{-1}), but a higher coulombic efficiency (90.7%). A higher coulombic efficiency in the cell with SiO_2-modified $LiNi_{0.5}Mn_{1.5}O_4$ electrodes suggests that the cross-linked composite polymer layer containing SiO_2 nanoparticles can effectively suppress the oxidative decomposition of the organic electrolyte on the $LiNi_{0.5}Mn_{1.5}O_4$ electrode at a high voltage

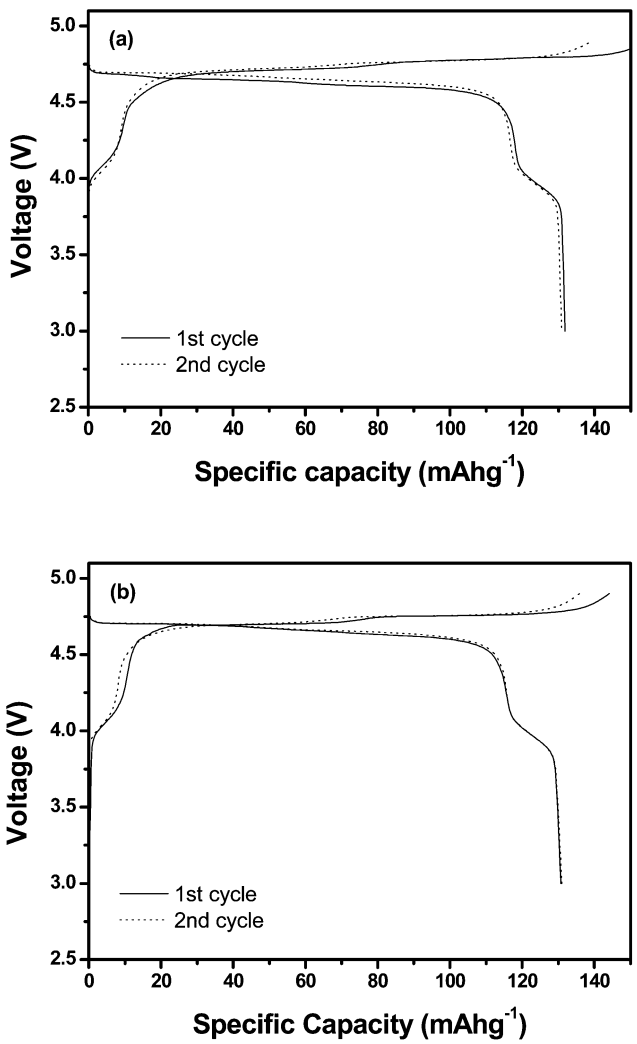

Fig. 6 Initial charge and discharge curves of the $Li/LiNi_{0.5}Mn_{1.5}O_4$ cells prepared with the (a) pristine $LiNi_{0.5}Mn_{1.5}O_4$ electrode and (b) SiO_2-modified $LiNi_{0.5}Mn_{1.5}O_4$ electrode (3 wt%).

(~4.9 V). For the second cycle, the coulombic efficiency of the Li/$LiNi_{0.5}Mn_{1.5}O_4$ cell with SiO_2-modified $LiNi_{0.5}Mn_{1.5}O_4$ electrode (96.4%) was still higher than that of the cell with the pristine $LiNi_{0.5}Mn_{1.5}O_4$ electrode (94.1%), indicating that the modified $LiNi_{0.5}Mn_{1.5}O_4$ electrode enables more reversible charge/discharge behavior.

The cycling performance of the Li/$LiNi_{0.5}Mn_{1.5}O_4$ cells was evaluated at a 0.5 C rate for both charge (constant-current and constant-voltage mode) and discharge (constant-current mode) in the voltage range of 3.0–4.9 V at 25 and 55 °C, respectively. As shown in Fig. 7(a), the capacity retention was improved in the cell with the SiO_2-modified $LiNi_{0.5}Mn_{1.5}O_4$ electrodes. The capacity retention of the pristine and modified $LiNi_{0.5}Mn_{1.5}O_4$ electrode (3 wt% SiO_2) was determined to be 77.0% and 83.9%, respectively. The coulombic efficiency increased with the content of reactive SiO_2 particles, as shown in Fig. S3.† This result suggests that the surface layer formed by reactive SiO_2 particles on $LiNi_{0.5}Mn_{1.5}O_4$ plays a role as a protective layer to cover the active cathode sites and reduce the oxidative decomposition of the electrolyte during cycling. At 55 °C, the cell with the pristine $LiNi_{0.5}Mn_{1.5}O_4$ electrode suffered from severe capacity fading after 50 cycles, resulting in a low discharge capacity of 72.3 mA h g^{-1} at the 100th cycle, as shown in Fig. 7(b). The poor cycling stability of the pristine $LiNi_{0.5}Mn_{1.5}O_4$ electrode at high temperatures can be ascribed to the dissolution of transition metals into the electrolyte as well as the oxidative decomposition of the electrolyte on the surface of the $LiNi_{0.5}Mn_{1.5}O_4$ electrode.[22–29] In contrast, the cells with the modified $LiNi_{0.5}Mn_{1.5}O_4$ electrode exhibited improved capacity retention. It is plausible that the cross-linked composite polymer layer containing SiO_2 particles, which are formed on the surface of $LiNi_{0.5}Mn_{1.5}O_4$ materials, is effective in protecting the active $LiNi_{0.5}Mn_{1.5}O_4$ materials from HF attack, resulting in suppression of Mn and Ni dissolution into the electrolyte. With respect to the effect of SiO_2 content on cycling behavior, the cell prepared with the modified $LiNi_{0.5}Mn_{1.5}O_4$ electrode containing 3 wt% SiO_2 showed the best capacity retention.

Fig. 8 shows the AC impedance spectra of the Li/$LiNi_{0.5}Mn_{1.5}O_4$ cells, which were obtained at a charged state after 100 cycles at 55 °C. All spectra exhibited two overlapping semicircles, which can be ascribed to the resistance of Li^+ ions through the SEI film (R_{SEI}) at the electrode surface, and to the charge transfer resistance at the electrode–electrolyte interface (R_{ct}).[30,31] Both R_{SEI} and R_{ct} are the largest in the cell with the pristine $LiNi_{0.5}Mn_{1.5}O_4$ electrode. This result may be associated with electrolyte decomposition and dissolution of transition metals due to insufficient protection for $LiNi_{0.5}Mn_{1.5}O_4$ active materials. As a result, the resistive SEI was developed on the $LiNi_{0.5}Mn_{1.5}O_4$ active material, and the charge transfer kinetics significantly deteriorated. On the other hand, the cross-linked composite polymer layer containing SiO_2 particles effectively prevented the direct exposure of the active $LiNi_{0.5}Mn_{1.5}O_4$ material to the liquid electrolyte; therefore, the harmful reactions between the $LiNi_{0.5}Mn_{1.5}O_4$ electrode and liquid

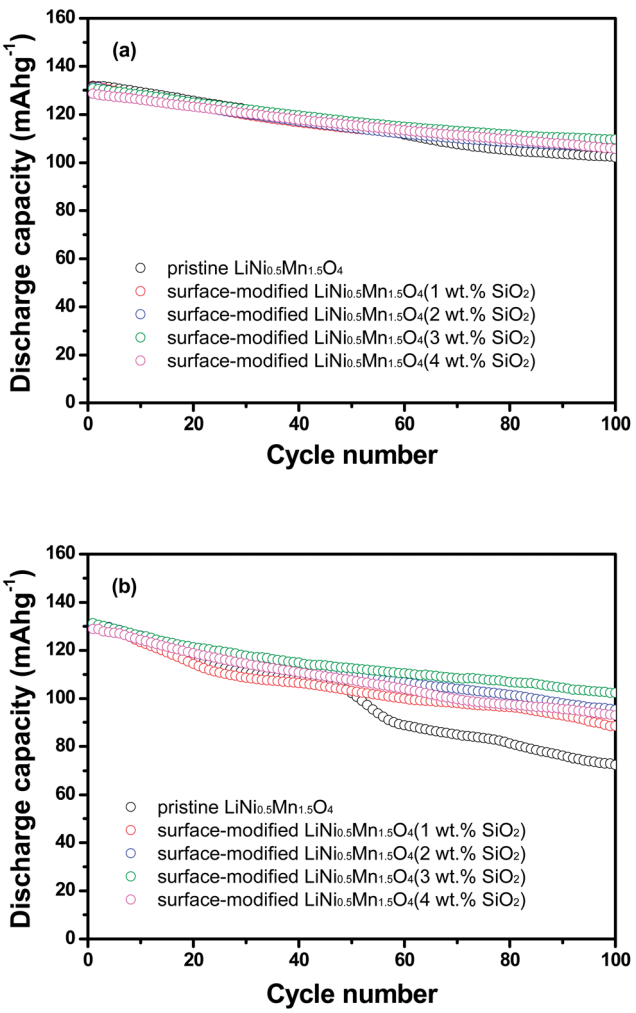

Fig. 7 Discharge capacities of the Li/$LiNi_{0.5}Mn_{1.5}O_4$ cells assembled with the pristine $LiNi_{0.5}Mn_{1.5}O_4$ electrode and SiO_2-modified $LiNi_{0.5}Mn_{1.5}O_4$ electrodes, which were cycled at (a) 25 °C and (b) 55 °C (0.5 C CC and CV charge, 0.5 C CC discharge, cut-off: 3.0–4.9 V).

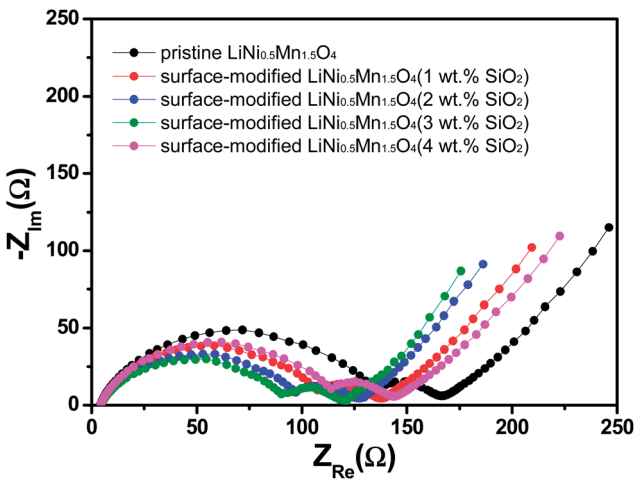

Fig. 8 AC impedance spectra of Li/$LiNi_{0.5}Mn_{1.5}O_4$ cells assembled with the pristine $LiNi_{0.5}Mn_{1.5}O_4$ electrode and SiO_2-modified $LiNi_{0.5}Mn_{1.5}O_4$ electrode, which were measured after the 100th cycling at 55 °C.

electrolyte could be alleviated, which resulted in lower interfacial resistances. Fig. S4† compares the cycling performance of the Li/$LiNi_{0.5}Mn_{1.5}O_4$ cells at different current rates. The relative capacity is defined as the ratio of the discharge capacity at a specific C rate to the discharge capacity delivered at a 0.2 C rate. Clearly, the Li/$LiNi_{0.5}Mn_{1.5}O_4$ cell assembled with 3 wt% SiO_2 exhibited the best cycling performance. As discussed earlier, the improvement of cycling stability with increasing SiO_2 content is due to the protective surface layer formed by reactive SiO_2 particles, which can suppress the oxidative decomposition of the electrolyte during cycling. However, the cross-linking with a large amount of reactive SiO_2 particles can cause the increase of resistance for ion migration in the surface layer formed on $LiNi_{0.5}Mn_{1.5}O_4$ particles (Fig. S2†), which gives rise to a reduction of discharge capacity at high current rates. Thus, the optimum content of reactive SiO_2 particles to ensure both cycling stability and high rate capability is 3 wt%.

To investigate the dissolution behavior of transition metals from the charged $LiNi_{0.5}Mn_{1.5}O_4$ electrode, the dissolved amounts of Mn and Ni were measured as a function of storage time at 55 °C. Fig. 9 shows that the dissolved amounts of Mn and Ni continuously increased with storage time for both pristine and SiO_2-modified $LiNi_{0.5}Mn_{1.5}O_4$ electrodes. The dissolution of Mn and Ni was due to the attack of HF generated as the hydrolysis product of $LiPF_6$ by a small amount of water in the liquid electrolyte.[32] The cycling stability of the SiO_2-modified $LiNi_{0.5}Mn_{1.5}O_4$ electrode at elevated temperature was good, considering the transition metals in the SiO_2-modified electrodes dissolved quite a bit into the electrolyte. It should be noted that the amount of electrolyte used in the experiment was quite high, as compared to the amount of electrolyte in the Li/$LiNi_{0.5}Mn_{1.5}O_4$ cell, which may cause the dissolution of a larger amount of transition metals into the liquid electrolyte. The pristine $LiNi_{0.5}Mn_{1.5}O_4$ electrode showed higher dissolution of Mn and Ni after 3 weeks, whereas smaller amounts of Mn and Ni were dissolved from the SiO_2-modified $LiNi_{0.5}Mn_{1.5}O_4$ electrodes. The dissolution of Mn and Ni reduced with the increasing content of reactive SiO_2 particles. Therefore, the cross-linked composite polymer layer with SiO_2 particles was effective in suppressing the dissolution of Mn and Ni by HF attack in the electrolyte. The SiO_2 particle itself was also expected to prevent structure disruption of active $LiNi_{0.5}Mn_{1.5}O_4$ materials and to protect $LiNi_{0.5}Mn_{1.5}O_4$ particles from the harmful side reactions, as previously reported.[33,34] As a result, the Li/$LiNi_{0.5}Mn_{1.5}O_4$ cells with SiO_2-modified $LiNi_{0.5}Mn_{1.5}O_4$ electrodes exhibited better cycling stability at elevated temperatures.

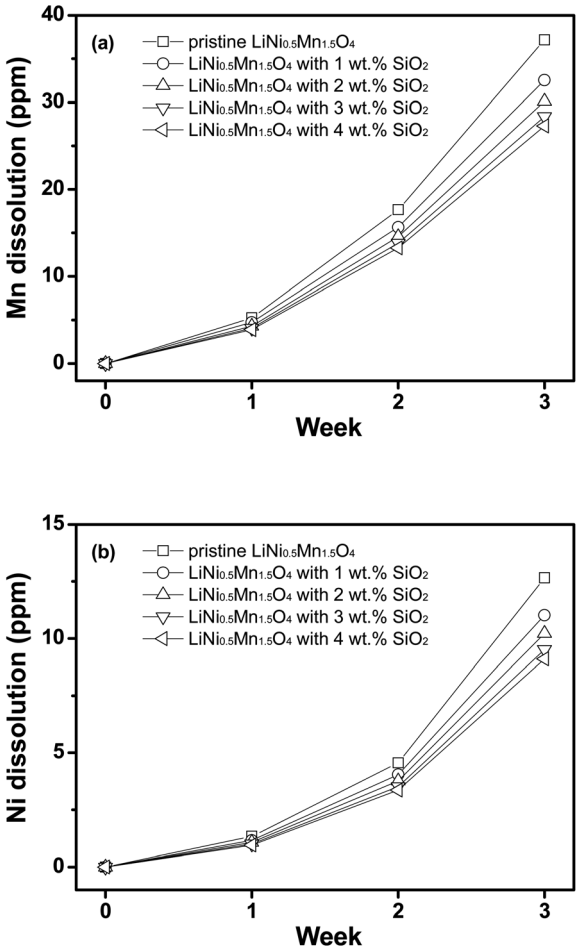

Fig. 9 (a) Mn and (b) Ni dissolution from the charged $LiNi_{0.5}Mn_{1.5}O_4$ electrodes into the liquid electrolyte as a function of storage time at 55 °C.

Conclusions

SiO_2 nanoparticles with reactive vinyl groups were synthesized and homogeneously dispersed on the surface of spinel $LiNi_{0.5}Mn_{1.5}O_4$ cathode materials. The $LiNi_{0.5}Mn_{1.5}O_4$ particles were then successfully wrapped by a cross-linked composite polymer layer formed by radical polymerization between reactive SiO_2 nanoparticles and DEGDA. The composite polymer layer with highly continuous surface coverage effectively served as a protective skin to suppress both the undesired interfacial reactions occurring on the $LiNi_{0.5}Mn_{1.5}O_4$ surface and the dissolution of transition metals from the charged $LiNi_{0.5}Mn_{1.5}O_4$ particles into the electrolyte solution at high temperatures. As a result, the cycling stability of the SiO_2-modified $LiNi_{0.5}Mn_{1.5}O_4$ electrodes was improved compared to the cell with the pristine $LiNi_{0.5}Mn_{1.5}O_4$ electrodes at high temperatures.

Acknowledgements

This work was supported by a grant from the Fundamental R&D Program for Core Technology of Materials and a Human Resources Development of KETEP grant funded by the Korean government Ministry of Trade, Industry and Energy (no. 20124010203290).

References

1 Z. Yang, J. Zhang, M. C. W. Kintner-Meyer, X. Lu, D. Choi, J. P. Lemmon and J. Liu, *Chem. Rev.*, 2011, **111**, 3577.
2 V. Etacheri, R. Marom, R. Elazari, G. Salitra and D. Aurbach, *Energy Environ. Sci.*, 2011, **4**, 3243.

3 M. M. Thackeray, C. Wolverton and E. D. Isaacs, *Energy Environ. Sci.*, 2012, **5**, 7854.
4 M. S. Whittingham, *Chem. Rev.*, 2004, **104**, 4271.
5 M. Mohamedi, M. Makino, K. Dokko, T. Itoh and I. Uchida, *Electrochim. Acta*, 2002, **48**, 79.
6 Y. Shin and A. Manthiram, *Electrochim. Acta*, 2003, **48**, 3583.
7 M. H. Lee, Y. J. Kang, S. T. Myung and Y. K. Sun, *Electrochim. Acta*, 2004, **50**, 939.
8 Y. Sun, Y. Yang, H. Zhan, H. Shao and Y. Zhou, *J. Power Sources*, 2010, **195**, 4322.
9 V. Borgel, E. Markevich, D. Aurbach, G. Semrau and M. Schmidt, *J. Power Sources*, 2009, **189**, 331.
10 R. Marom, S. F. Amalraj, N. Leifer, D. Jacob and D. Aurbach, *J. Mater. Chem.*, 2011, **21**, 9938.
11 J. N. Lee, G. B. Han, M. H. Ryou, D. J. Lee, J. C. Song, J. W. Choi and J. K. Park, *Electrochim. Acta*, 2011, **56**, 5195.
12 Y. K. Sun, K. J. Hong, J. Prakash and K. Amine, *Electrochem. Commun.*, 2002, **4**, 344.
13 Y. Kobayashi, H. Miyashiro, K. Takei, H. Shigemura, M. Tabuchi, H. Kageyama and T. Iwahori, *J. Electrochem. Soc.*, 2003, **150**, A1577.
14 S. T. Myung, K. Amine and Y. K. Sun, *J. Mater. Chem.*, 2010, **20**, 7074.
15 H. B. Kang, S. T. Myung, K. Amine, S. M. Lee and Y. K. Sun, *J. Power Sources*, 2010, **195**, 2023.
16 S. E. Cheon, C. W. Kwon, D. B. Kim, S. J. Hong, H. T. Kim and S. W. Kim, *Electrochim. Acta*, 2000, **46**, 599.
17 J. H. Cho, J. H. Park, M. H. Lee, H. K. Song and S. Y. Lee, *Energy Environ. Sci.*, 2012, **5**, 7124.
18 Y. S. Lee, S. H. Ju, J. H. Kim, S. S. Hwang, J. M. Choi, Y. K. Sun, H. Kim, B. Scrosati and D. W. Kim, *Electrochem. Commun.*, 2012, **17**, 18.
19 S. H. Ju, Y. S. Lee, Y. K. Sun and D. W. Kim, *J. Mater. Chem. A*, 2013, **1**, 395.
20 Y. S. Lee, J. H. Lee, J. A. Choi, W. Y. Yoon and D. W. Kim, *Adv. Funct. Mater.*, 2013, **23**, 1019.
21 M. M. Thackeray, W. I. F. David, P. G. Bruce and J. B. Goodenough, *Mater. Res. Bull.*, 1983, **18**, 461.
22 B. J. Hwang, R. Santhanam, D. G. Liu and Y. W. Tsai, *J. Power Sources*, 2001, **102**, 326.
23 Y. K. Sun, C. S. Yoon and I. H. Oh, *Electrochim. Acta*, 2003, **48**, 503.
24 J. Arrebola, A. Caballero, L. Hernan, J. Morales, E. R. Castellon and J. R. R. Barrado, *J. Electrochem. Soc.*, 2007, **154**, A178.
25 J. Liu and A. Manthiram, *J. Phys. Chem. C*, 2009, **113**, 15073.
26 J. Liu and A. Manthiram, *J. Electrochem. Soc.*, 2009, **156**, A66.
27 H. M. Wu, I. Belharouak, A. Abouimrane, Y. K. Sun and K. Amine, *J. Power Sources*, 2010, **195**, 2909.
28 H. Deng, I. Belharouak, C. S. Yoon, Y. K. Sun and K. Amine, *J. Electrochem. Soc.*, 2010, **157**, A1035.
29 D. J. Lee, K. S. Lee, S. T. Myung, H. Yashiro and Y. K. Sun, *J. Power Sources*, 2011, **196**, 1353.
30 A. Funabiki, M. Inaba and Z. Ogumi, *J. Power Sources*, 1997, **68**, 227.
31 M. D. Levi, G. Salitra, B. Markovsky, H. Teller, D. Aurbach, U. Heider and L. Heider, *J. Electrochem. Soc.*, 1999, **146**, 1279.
32 K. Tasaki, A. Goldberg, J. J. Lian, M. Walker, A. Timmons and S. J. Harris, *J. Electrochem. Soc.*, 2009, **156**, A1019.
33 R. Alcantara, M. Jaraba, P. Lavela and J. L. Tirado, *J. Electroanal. Chem.*, 2004, **566**, 187.
34 A. Eftekhari, *Chem. Lett.*, 2004, **33**, 616.